Available online at www.sciencedirect.com
ScienceDirect
Inorganica Chimica Acta 360 (2007) 1599–1608
Inorganica Chimica Acta
www.elsevier.com/locate/ica

Hydrazone Schiff base-manganese(II) complexes: Synthesis, crystal structure and catalytic reactivity

Omid Pouralimardan [a], Anne-Christine Chamayou [b], Christoph Janiak [b], Hassan Hosseini-Monfared [a,*]

[a] Department of Chemistry, Faculty of Sciences, Zanjan University, Zanjan 45195-313, Iran
[b] Institut für Anorganische und Analytische Chemie, Universität Freiburg, Albertstrasse 21, 79104 Freiburg, Germany

Received 11 June 2006; received in revised form 27 August 2006; accepted 28 August 2006
Available online 23 September 2006

Abstract

Five dissymmetric tridentate Schiff base ligands, containing a mixed donor set of ONN and ONO were prepared by the reaction of benzhydrazide with the appropriate salicylaldehyde and pyridine-2-carbaldehyde and characterized by FT-IR, ^{1}H and ^{13}C NMR. The complexes of these ligands were synthesized by treating an ethanolic solution of the appropriate ligand and one equivalent Et_3N with an equimolar amount of $MnCl_2 \cdot 4H_2O$ or alternatively by a more direct route in which an ethanolic solution of benzhydrazide was added to ethanolic solution of appropriate salicylaldehyde and $MnCl_2 \cdot 4H_2O$ solution to yield $[MnCl(L^1)(H_2O)_2]$, $[Mn(L^2)_2(H_2O)_2]$, $[MnCl(L^3)]$, $[MnCl(L^4)]$ and $[MnCl_2(H_2O)(L^5)]$. The hydrazone Schiff base ligands and their manganese complexes including HL^{1-4} and L^5 (HL^1 = benzoic acid (2-hydroxy-3-methoxy-benzylidene)-hydrazide, HL^2 = benzoic acid (2,3-dihydroxy-benzylidene)-hydrazide, HL^3 = benzoic acid (2-hydroxy-benzylidene)-hydrazide, HL^4 = benzoic acid (5-bromo-2-hydroxy-benzylidene)-hydrazide, L^5 = benzoic acid pyridine-2-yl methylene-hydrazide) were characterized on the basis of their FT-IR, ^{1}H and ^{13}C NMR, and molar conductivity. The crystal structures of HL^1 and $[MnCl_2(H_2O)L^5]$ have been determined. The results suggest that the Schiff bases HL^1, HL^2, HL^3, and HL^4 coordinate as univalent anions with their tridentate O,N,O donors derived from the carbonyl and phenolic oxygen and azomethine nitrogen. L^5 is a neutral tridentate Schiff base with N,N,O donors. ESI-MS for the complexes Mn–$L^{2,3,5}$ provided evidence for the presence of multinuclear complexes in solution. Catalytic ability of Mn–L^{1-5} complexes were examined and found that highly selective epoxidation (>95%) of cyclohexene was performed by iodosylbenzene in the presence of these complexes and imidazole in acetonitrile.

Keywords: Crystal structure; Dissymmetric Schiff base; Hydrazone; Manganese complexes; Oxidation

1. Introduction

The finding of efficient catalysts for the selective insertion of one oxygen atom from oxygen donors, like iodosylbenzene, dioxygen, hydrogen peroxide, alkylhydroperoxide, or sodium hypochlorite into various organic molecules, under mild conditions, remains a difficult challenge in the fields of chemical and biological catalysis [1,2]. The oxidation of hydrocarbons by transition metal complexes has been studied extensively [3–9].

Among the inorganic mimics of enzymes, metal complexes containing porphyrin, salen (salen = *N*,*N*′-ethylene-bis(salicylideneaminato), and phthalocyanine ligands have been investigated as possible alternative catalysts in many oxidation and hydroxylation reactions [10–14]. Salen ligands give complexes which in addition to alkene epoxidation also hold promise in enantioselective cyclopropanation of styrenes, asymmetric aziridination of olefins, asymmetric Diels–Alder cycloaddition, and enantioselective ring opening of epoxides [15]. Generally, the electronic

* Corresponding author. Tel.: +98 241 5152576; fax: +98 241 5283203.
E-mail addresses: monfared@mail.znu.ac.ir, monfared_2@yahoo.com (H. Hosseini-Monfared).

0020-1693/$ - see front matter © 2006 Elsevier B.V. All rights reserved.
doi:10.1016/j.ica.2006.08.056

and structural properties of the ligands play an important role in the catalytic properties [16]. In the symmetric salen Schiff base complexes studied to date, the two identical salicylaldehyde moieties on both sides of the diamine in the ligands make the same electronic and steric contributions. The obvious difficulty in the synthesis of non-symmetrical Salen ligands is that the straight condensation methodology used for symmetrical salen ligands is no longer applicable. Unsymmetrical combination allows tuning both the electronic properties from one side and the steric effects from the other side simultaneously and collectively to maximize the performance of the non-symmetrical Schiff base catalysts. Unsymmetrical Schiff base can bind with one, two or more metal centers involving various coordination modes and allow successful synthesis of homo and/or heteronuclear metal complexes with interesting stereochemistry [17–20].

Non-symmetrical salen-type ligands (Scheme 1a) has some similarities to the product of salicylaldehyde and benzhydrazide condensation (Scheme 1b). While salen-type ligands act as a four dentate chelating agents, because of short N–N bound and molecular conformation we expect benzhydrazone to act mainly as tridentate chelating ligand or four dentate bridging ligands. However, they have similarities in donor atoms and we predicted that these types of hydrazone Schiff base complexes must show considerable catalytic activities in oxidation of alkenes.

In analytical chemistry hydrazones find application by acting as multidentate ligands [21,22] with metals (usually from the transition group). Various studies have also shown that the azomethine group having a lone pair of electrons in either a π or sp^2 hybridized orbital on trigonally hybridized nitrogen has considerable biological importance [23]. Hydrazone complexes of Cu(II), Ni(II), Pd(II) [24] and Co(II) [25–27] and benzoylhydrazone complexes of copper(II) [28], vanadium [29,30], and ruthenium(II) [31] have been studied.

The present work deals with the synthesis and characterization by physical methods of the ligands obtained in the reaction of benzhydrazide with some carbonyl compounds, manganese complexes of these ligands, and catalytic oxidation of alkenes in the presence of these complexes. The crystal structure of one of these ligands and one manganese complexes were also determined.

There has been interest in the design, synthesis and application of non-symmetric Schiff base ligands. This has been stimulated from the awareness that in many metalloproteins the metals are contained in non-symmetrical

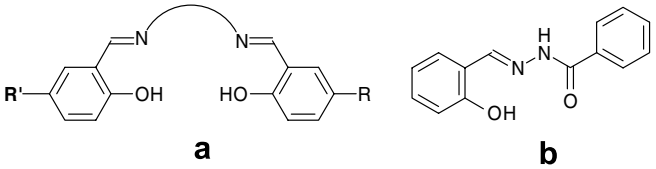

Scheme 1. Similarity between a non-symmetrical salen-type ligand and benzhydrazide Schiff base ligand.

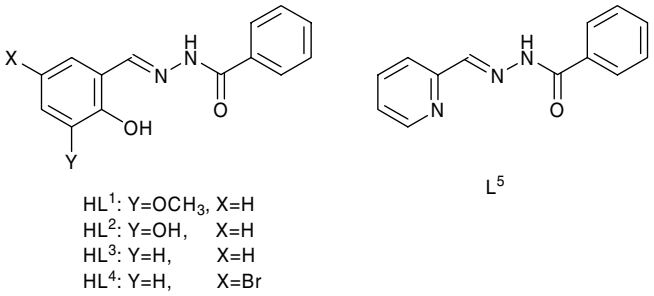

HL^1: Y=OCH_3, X=H
HL^2: Y=OH, X=H
HL^3: Y=H, X=H
HL^4: Y=H, X=Br

Scheme 2. Tridentate hydrazone Schiff base ligands.

environments and also by an interest in the potential modification of the properties of complexes derived from ligands having present non-symmetrical mixed sets of donor atoms [32,33].

2. Experimental

Benzhydrazide, salicylaldehyde, 2-pyridine carbaldehyde, imidazole, cyclohexene, $MnCl_2 \cdot 4H_2O$, and solvents with high purity were purchased from Merck. Cyclohexene purity was checked by gas chromatographic analysis before using. PhIO [34] was synthesized according to the reported procedures. Other materials were purchased in the highest possible purity and used as received.

IR spectra were recorded in KBr disks with a Matson 1000 FT-IR spectrophotometer. UV–Vis spectra of solution were recorded on a Shimadzu 160 spectrometer. ^1H and ^{13}C NMR spectra of ligands in DMSO-d_6 solution were recorded on a Bruker 250 MHz spectrometer and chemical shifts are indicated in ppm relative to tetramethylsilane. The reaction products of oxidation were determined and analyzed by HP Agilent 6890 gas chromatograph equipped with a HP-5 capillary column (phenyl methyl siloxane 30 m × 320 μm × 0.25 μm) and flame-ionization detector. The elemental analysis (carbon, hydrogen, and nitrogen) of compounds were obtained from Carlo ERBA Model EA 1108 analyzer. Molar conductivities were determined with a Metrohm 644 conductometer. Manganese percentages of complexes were measured by a Varian spectrometer AAS-110. Electron spray ionization mass spectra (ESI-MS) were collected using a Finnigan MAT LCQ Advantage. MeOH was used as the solvent with and without TFA (CF_3COOH, 0.06% in MeCN) added. Mass spectra were measured in positive mode and in the range $m/z = 200$–1400.

2.1. Synthesis of ligands

General procedure: All ligands were prepared in a similar manner according to the reported procedures [35,36], and here the synthesis of HL^3 is given.

To a methanol solution (10 ml) of benzhydrazide (136 mg, 1 mmol), methanol (10 ml) solution of salicylaldehyde (122 mg, 1 mmol) was drop wise added and the mixture was refluxed for 2 h. The solution was then evaporated

on a steam bath to 5 cm^3 and cooled to room temperature. Yellow crystals separated and were filtered off, washed with 5 ml of cooled methanol and then dried in air. The analytical and physical data of the ligands are given in Table 2.

2.2. Synthesis of metal complexes: method-a

General procedure: The appropriate ligand (HL^1, HL^2, HL^3or HL^4) (1.2 mmol) was dissolved in absolute ethanol (10 ml) containing Et_3N (0.12 g, 1.2 mmol). $MnCl_2 \cdot 4H_2O$ (0.24 g, 1.2 mmol) was added and the solution was gently refluxed for 4 h. After cooling, the resulting solid was filtered off, washed with cooled absolute ethanol, recrystallized from methanol/ethanol (50:50 v/v) and then dried at 100 °C. The analytical and physical data of the complexes are given in Table 2.

2.3. Synthesis of metal complexes: method-b

For example for Mn–L^5: to a solution of pyridine-2-carbaldehyde (0.535 g, 5 mmol) in absolute ethanol (15 ml), $MnCl_2 \cdot 4H_2O$ (0.98 g, 5 mmol) was added. The mixture was stirred at room temperature for 30 min and then ethanol solution (10 ml) of benzhydrazide (0.68 g, 5 mmol) was added. The reaction mixture was stirred under reflux for 3 h. The obtained yellow colored solution was cooled to room temperature. The product was removed by filtration, washed with cooled absolute ethanol, recrystallized from methanol/ethanol (50:50 v/v) and dried in air.

2.4. X-ray crystallography

X-ray quality crystals of HL^1 and $[MnCl_2(H_2O)(L^5)]$ could be grown from methanol and ethanol, respectively.

Data collection: Bruker AXS with CCD area-detector, temperature 293(2) K, Mo Kα radiation ($\lambda = 0.71073$ Å), graphite monochromator, ω-scans, Data collection and cell refinement with SMART [37], data reduction with SAINT [37], experimental absorption correction with SADABS [38]. *Structure analysis and refinement*: The structure was solved by direct methods (SHELXS-97) [39]; refinement was done by full-matrix least-squares on F^2 using the SHELXL-97 program suite [39]. Both HL^1 (as the hydrate) and $[MnCl_2(H_2O)(L^5)]$ were found to crystallize in non-centrosymmetric space groups. For $HL^1 \cdot H_2O$ the absolute structure or Flack-parameter is, however, meaningless in the absence of a heavy atom and the use of anomalous dispersion so that the correct absolute structure or twin law could not be determined. The structure of $[MnCl_2(H_2O)(L^5)]$ was refined as a racemic twin (twin law $-100\ 0-10\ 00-1$)

Table 1
Crystal data and structure refinement for $HL^1 \cdot H_2O$ and $[MnCl_2(H_2O)(L^5)]$

Compound	$HL^1 \cdot H_2O$	$[MnCl_2(H_2O)(L^5)]$
Empirical formula	$C_{15}H_{16}N_2O_4$	$C_{13}H_{13}Cl_2MnN_3O_2$
Molecular weight (g mol^{-1})	288.30	369.10
Crystal size (mm)	$0.90 \times 0.13 \times 0.09$	$0.26 \times 0.12 \times 0.07$
Crystal appearance	needle, transparent	isomorphous, yellow
2θ Range (°)	3.66–55.38	4.70–54.70
h; *k*; *l* Range	−6, 6; −16, 16; −27, 28	−22, 22; −8, 9; −15, 16
Crystal system	orthorhombic	orthorhombic
Space group	$P2_12_12_1$	$Pca2_1$
a (Å)	5.0118(11)	17.304(5)
b (Å)	12.919(3)	7.152(2)
c (Å)	21.910(5)	12.469(3)
V (Å^3)	1418.5(5)	1543.1(7)
Z	4	4
D_{calc} (g cm^{-3})	1.350	1.589
F(000)	608	748
μ (mm^{-1})	0.099	1.207
Maximum/minimum transmission	0.9907/0.9160	0.9160/0.7467
Reflections collected	12694	12871
Independent reflections (R_{int})	3264 (0.0357)	3469 (0.0535)
Observed reflections [$I > 2\sigma(I)$]	1951	2386
Parameters refined	206	200
Maximum/minimum $\Delta\rho$[a] (e Å^{-3})	0.123/−0.153	0.592/−0.440
R_1/wR_2 [$I > 2\sigma(I)$][b]	0.0349/0.0769	0.0392/0.0723
R_1/wR_2 (all reflections)[b]	0.0814/0.0918	0.0821/0.0884
Goodness-of-fit (GOF) on F^2[c]	0.956	1.054
Weighting scheme *w*; *a*/*b*[d]	0.0455/0.0000	0.0229/0.0000
Absolute structure parameter (Flack value[e])	not applicable	0.0(3)

[a] Largest difference in peak and hole.
[b] $R_1 = [\sum(\|F_o| - |F_c\|)/\sum|F_o|]$; $wR_2 = [\sum[w(F_o^2 - F_c^2)^2]/\sum[w(F_o^2)^2]]^{1/2}$.
[c] GOF $= [\sum[w(F_o^2 - F_c^2)^2]/(n-p)]^{1/2}$.
[d] $w = 1/[\sum^2(F_o^2) + (aP)^2 + bP]$ where $P = (\max(F_o^2 \text{ or } 0) + 2F_c^2)/3$.
[e] H.D. Flack, Acta Crystallogr., Sect. A 39 (1983) 876–881.

Table 2
Analytical and physical data of the ligands and their complexes

Compound	Empirical formula (formula weight)	Yield (%)	Color	Melting point (°C)	Molar conductivity (Ω^{-1} cm^2 mol^{-1})	Analyses found (Calc.) (%)			
						C	H	N	Mn
HL^1	$C_{15}H_{14}N_2O_3$ (270.28)	86	yellow	195		66.60 (66.66)	5.30 (5.22)	10.29 (10.36)	
HL^2	$C_{14}H_{12}N_2O_3$ (256.26)	80	brown	208		65.70 (65.61)	4.70 (4.73)	11.00 (10.93)	
HL^3	$C_{14}H_{12}N_2O_2$ (240.26)	90	yellow	172		69.89 (69.99)	5.00 (5.03)	11.59 (11.66)	
HL^4	$C_{14}H_{11}BrN_2O_2$ (319.15)	85	light yellow	199–204		52.71 (52.69)	3.40 (3.47)	8.81 (8.78)	
L^5	$C_{13}H_{11}N_3O$ (225.26)	78	brown	waxy		69.40 (69.31)	4.88 (4.93)	18.80 (18.65)	
Mn–L^1	$[MnCl(L^1)(H_2O)_2]$ (395.70)	80	yellow		3.1	45.44 (45.53)	4.31 (4.33)	6.33 (7.08)	14.00 (13.88)
Mn–L^2	$[Mn(L^2)_2(H_2O)_2]$ (601.48)	33	yellow		11.4	55.29 (55.91)	3.74 (4.37)	8.79 (9.32)	9.73 (9.13)
Mn–L^3	$[MnCl(L^3)]$ (329.64)	35	yellow		4.0	50.92 (51.01)	2.71 (3.37)	8.60 (8.50)	16.57 (16.67)
Mn–L^4	$[MnCl(L^4)]$ (408.53)	79	yellow		15.2	41.76 (41.16)	1.37 (2.47)	7.04 (6.86)	13.86 (13.45)
Mn–L^5	$[MnCl_2(H_2O)(L^5)]$ (369.10)	53	yellow		28	43.30 (42.30)	2.43 (3.01)	11.78 (11.39)	15.50 (14.88)

(BASF = 0.45320). All non-hydrogen positions were found and refined with anisotropic temperature factors. Hydrogen atoms on oxygen (–OH) and nitrogen (–NH–Ph, $–NH_2$) were found and freely refined in $HL^1 \cdot H_2O$ and with $U_{eq}(H) = 1.2U_{eq}(N)$ and $U_{eq}(H) = 1.5U_{eq}(O)$ in $[MnCl_2(H_2O)(L^5)]$. Hydrogen atoms on C (phenyl and CH_3) were calculated with appropriate riding models (AFIX 43 and 33, respectively) and $U_{eq}(H) = 1.2U_{eq}(C)$ (CH) or $U_{eq}(H) = 1.5U_{eq}(C)$ (CH_3). Details of the X-ray structure determinations and refinements are provided in Table 1. Graphics were drawn with DIAMOND (Version 3.1b) [40]. Computations on the supramolecular π-interactions were carried out with PLATON for Windows [41–43].

2.5. General oxidation procedure

Catalytic oxidations were performed in stirred flasks. In a typical experiment a mixture of 0.010 mmol catalyst, 3 ml solvent, 1 mmol cyclohexene, 0.1 mmol imidazole, and 0.175 mmol *n*-octane as internal standard, was prepared in a round-bottom flask. The flask was placed in a water bath at 32 ± 1 °C. To initiate the reaction, 0.50 mmol of iodosylbenzene was added. At appropriate intervals, aliquots were removed and analyzed immediately by GC. Oxidation products yields based on the oxidant, were quantified by comparison with *n*-octane.

3. Results and discussion

3.1. Synthesis of ligands and Mn-complexes

The reaction of benzhydrazide with several salicylaldehyde derivatives containing donor, withdrawing and bulky groups in methanol gave the desired dissymmetric tridentate Schiff base ligands in high yields and purity (Scheme 3).

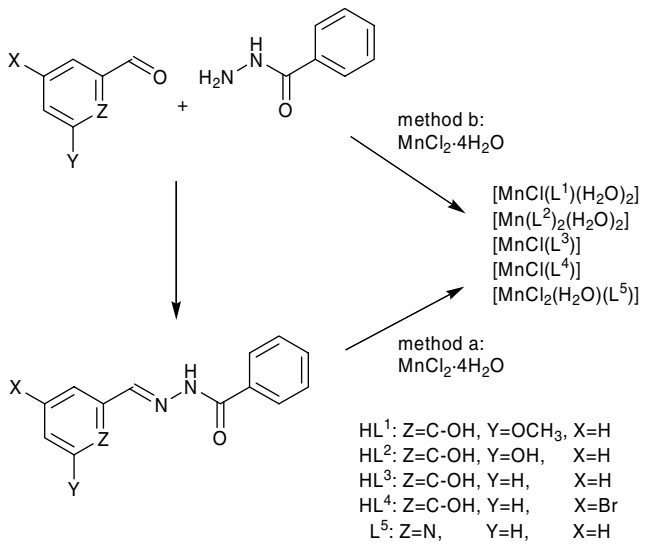

Scheme 3. Ligand and complex syntheses.

Table 3
^{1}H NMR of ligands HL^1–L^5

Compound	Solvent	–C*H*=N–	–N*H*–	–O*H*
HL^1	$(CD_3)_2SO$	8.64	12.09	10.96
HL^1	$(CD_3)_2SO + D_2O$	8.63		
HL^2	$(CD_3)_2SO$	8.59	12.03	9.09, 11.14
HL^2	$(CD_3)_2SO + D_2O$	8.56		
HL^3	$(CD_3)_2SO$	8.64	12.02	11.30
HL^3	$(CD_3)_2SO + D_2O$	8.60		
HL^4	$(CD_3)_2SO$	8.60	12.10	11.23
HL^4	$(CD_3)_2SO + D_2O$	8.59		
L^5	$(CD_3)_2SO$	8.60	12.09	
L^5	$(CD_3)_2SO + D_2O$	8.60		

Mn(II) complexes with tridentate hydrazone Schiff base ligands were prepared by treating an ethanolic solution of the appropriate ligand and one equivalent of Et_3N with an equimolar amount of $MnCl_2 \cdot 4H_2O$ or alternatively by a more direct route in which an ethanolic solution of benzhydrazide was added to an ethanolic solution of the appropriate salicylaldehyde and $MnCl_2 \cdot 4H_2O$ solution prior to any isolation. Both routes gave identical products but the latter was less time consuming and gave higher yields (Scheme 3).

The manganese complexes are soluble in methanol. Electrical conductivity measurements of Mn–L^{1-5} give Λ_M values of 3–28 Ω^{-1} cm^2 mol^{-1} and confirm that they are neutral and non-electrolytes [44].

^{1}H and ^{13}C NMR spectra data of the ligands in DMSO-d_6 (Tables 3 and 4) confirm the proposed structure of the ligands (Scheme 2). The principal peaks of the ^{1}H NMR spectra of ligands HL^1–L^5 are listed in Table 3.

Due to the complexity of the aromatic region (δ 8–6), no band assignments have been made for the aromatic protons. The signal at δ 12.02–12.10 in the spectra of HL^1–L^5 is assigned to the common NH-group, concomitant with the observation of a rapid loss of these signals when D_2O is added to the solution. Also the signals between δ 9.09–11.23 in the spectra of HL^1–HL^4 are lost upon addition of D_2O to the solution. Hence, this signal is assigned to the aromatic –OH group (two aromatic –OH groups in HL^2) which is not present in L^5. The resonances between δ 7.66–9.1 are assigned to the azomethine (–CH=N–) in the spectra of HL^1–L^5. In a study of ligands of somewhat similar type the azomethine resonance have been reported in the region δ 7–9 [25,26,45].

The main stretching frequencies of the IR spectra of the ligands (HL^1–L^5) and their complexes are tabulated in Table 5. The IR spectra of ligands and their corresponding complexes are found to be very similar to each other. Hence significant frequencies are selected by comparing the IR spectra of the ligands with those of manganese complexes. The very strong and sharp bands located at 1649–1673 cm^{-1} are assigned to the ν(C=N) stretching vibrations of azomethine of the ligands. These bands are shifted 27–66 cm^{-1} to lower wavenumber. These shifts to lower wavenumbers support the participation of the azomethine group of these ligands in binding to the manganese ion [25,26].

Infrared spectra of complexes display the characteristic bands associated with the N–H and C=O bonds of the amide functionality present in the free Schiff bases [46,47]. The N–H broad bands at 3378–3393 cm^{-1} and 3209–3262 cm^{-1} in the ligands are found at 3354 cm^{-1} and 3124–3247 cm^{-1} in the complexes. Thus in each complex the amide functionality exists and is not deprotonated. The IR spectra of ligands display bands at 1557–1612 cm^{-1} and 1466–1473 cm^{-1}. These bands are assigned to the C=O of amide functionality. After complexation, they are shifted to lower wavenumbers 1543–1569 cm^{-1} and 1392–1473 cm^{-1} and these findings support involvement of C=O in coordination to manganese ion.

In addition a broad band (for HL^1 sharp) is centered at 3424–3586 cm^{-1} in HL^1–HL^4 due to the O–H of the phenol, probably involved in intramolecular hydrogen bonding. Absence of the phenolic O–H vibration indicates that it is deprotonated in complexes. Shift of C–O stretch of phenol to higher wavenumber confirms that manganese ion is bound to the phenolic oxygen. Very broad O–H vibration at 3438 and 3424 cm^{-1} in Mn–L^3 and Mn–L^4, are probably due to the adsorbed water molecule [47].

Most of the band shifts observed at the wave number region 1150–994 cm^{-1} is in agreement with the structural changes observed in the molecular carbon skeleton after complexation, which cause some important changes in (C–C) bond lengths. Comparison of IR spectra of the Mn–L^{1-5} complexes and the HL^1–L^5 ligands, indicate that in these ligands the azomethine N–H is still present and the phenolic O–H is deprotonated. It is suggested that the mono-anionic L^{1-4} ligands are also bound tridentate as

Table 4
^{13}C NMR data for ligands HL^1–L^5(ppm)

HL^1	HL^2	HL^3	HL^4	L^5
163.28, 148.67	163.28, 149.53	163.31, 157.95	163.45, 156.90	163.87, 153.72
148.40, 147.63	146.58, 146.06	148.82, 33.26	146.17, 134.01	149.96, 148.51
133.29, 132.42	133.23, 132.46	132.43, 31.84	133.18, 132.49	137.32, 133.65
129.00, 128.09	129.01, 128.10	130.02, 29.00	130.95, 128.99	132.41, 128.98
121.29, 119.49	120.58, 119.63	128.10, 19.80	128.14, 121.75	128.17, 124.84
119.36, 114.28	119.20, 117.87	119.11, 16.88	119.13, 110.90	120.37
56.27				

Table 5
Selected characteristic IR bands (4000–500 cm^{-1}) of HL^1–L^5 ligands and their complexes

Compound	ν(O–H)	ν(N–H)	ν(C=N)	ν(CO)	δ(C–H)
HL^1	3572s	3378s, br 3209s, br	1650vs	1573s 1473s	701s
Mn–L^1		3354s, br 3208s, br	1623vs	1569s 1451s	
HL^2	3486s, br	3231m, br	1649s	1557s 1472s	
Mn–L^2	3432vs, vbr	3247m, br	1609vs	1558vs 1443s	
HL^3	3447s, vbr	3262s, br	1673vs	1612s 1472s	
Mn–L^3	3438m, vbr	3165m, br	1607vs	1569s 1392m	
HL^4	3563s	3386s, vbr 3216m, br	1659vs	1574s 1466s	
Mn–L^4	3424m, vbr		1604vs	1566s 1457s	
L^5	3393s, vbr	3393s, vbr 3223	1665vs	1557s 1480s	632m
Mn–L^5		3124m, br	1627vs	1543vs 1473	623m

the neutral L^5 ligand in the structure of $[MnCl_2(H_2O)(L^5)]$. These IR findings indicate that L^1–L^4 behave as a mono-anionic ligands. L^5 is a neutral N,N,O tridentate chelating ligand in the manganese complex.

Methanol solutions of the complexes are yellow-orange in color. These solutions have been used to record the electronic spectra. The ligands and their complexes display three very similar absorptions in the 200–400 nm region with peaks around 230, 300–340 and 390 nm, so they are most likely due to transitions involving the ligand orbitals only.

From the electron spray ionization mass spectrometry data (ESI-MS) given in Table 6 for the complexes Mn–$L^{2,3,5}$ we suggest that multinuclear complexes are present in solution. Signals for Mn_2L_2 feature prominently. Dinuclear and tetranuclear manganese(III) chloro complexes have e.g. been found with salicylidenealdiminato or (pyridylmethyl)aminomethyl)phenolato ligands [48–51].

3.2. X-ray structures of $HL^1 \cdot H_2O$ and $[MnCl_2(H_2O)(L^5)]$

The compound HL^1 was found to crystallize as the monohydrate from single-crystal structural analysis. The molecular structure of $HL^1 \cdot H_2O$ with the hydrogen bonding interactions is shown in Fig. 1. HL^1 shows the expected

Table 6
ESI-MS data for complexes Mn–L^2, Mn–L^3 and Mn–L^5

Compound	Solvent		Assignment
	CH_3OH	CH_3OH in CH_3CN + 0.06% TFAH	
	m/z (intensity, %)		
Mn–L^2	323 (100)	323 (31)	$[L + 2H_2O + CH_3OH]^+$
$[Mn(L^2)_2(H_2O)_2]$		504 (36)	$[Mn_2OL^2 + 3CH_3CN]^+$
		671 (100)	$[Mn_2(L^2)_2 + 3OH^-]^+$ (Mn^{III})
	733 (90)		$[Mn_2(L^2)_2 + OH^- + 3CH_3OH]$
	875 (49)		$[Mn_2(L^2)_3]^+$
	1046 (82)		$[Mn_3O(L^2)_3 + 2H_2O + 2CH_3OH]^+$
	1189 (39)		$[Mn_4O_2(L^2)_3 + 6H_2O + 2CH_3OH]^+$
Mn–L^3		239 (38)	$[L^3 - H]^+$
$[MnCl(L^3)]$	240 (100)		$[L^3 + H^+]^+$
	326 (30)		$[ML^3 + CH_3OH]^+$
		335 (29)	$[ML^3 + CH_3CN]^+$
	358 (34)		$[ML^3 + 2CH_3OH]^+$
		376 (33)	$[ML^3 + 2CH_3CN]^+$
	534 (16)	534 (36)	$[M(L^3)_2 + H^+]^+$
	623 (34)	623 (100)	$[Mn_2(L^3)_2Cl]^+$ (Cl isotopic pattern)
		701 (44)	$[Mn_2(L^3)_2 + TFA^-]^+$
	748 (15)	748 (30)	$[Mn_3(L^3)_2Cl_3]^+$ (Cl_3 isotopic pattern)
Mn–L^5	311 (30)		$[ML^5 - H^+ + CH_3OH]^+$
$[MnCl_2(H_2O)(L^5)]$	343 (29)		$[ML^5 - H^+ + 2CH_3OH]^+$
		361 (41)	$[ML^5 + OH^- + 2CH_3OH]^+$
	504 (87)	504 (41)	$[M(L^5)_2 - H^+]^+$
	593 (40)	593 (42)	$[Mn_2(L^5)_2 - 2H^+ + H_2O + OH^-]^+$
		671 (62)	$[Mn_2(L^5)_2 - 2H^+ + TFA^-]^+$
	782 (100)	782 (100)	$[Mn_2(L^5)_3 - 3H^+]^+$
	907 (16)	907 (14)	$[Mn_3Cl_2(L^5)_3 - 3H^+]^+$ (Cl_2 isotopic pattern)

TFAH = CF_3COOH, note the equivalency $TFA^- = OH^- + 3CH_3OH$.

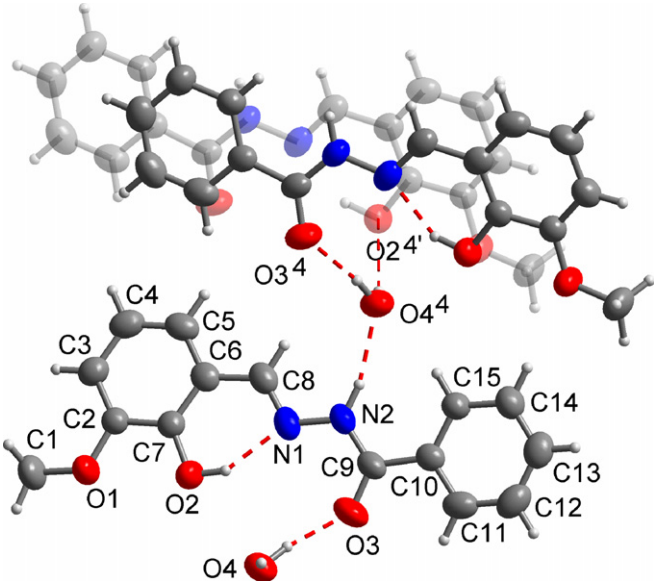

Fig. 1. Structure of $HL^1 \cdot H_2O$ with atom numbering and hydrogen bonding interactions. Ellipsoids are drawn with 50% probability. The two upper, partially overlayered molecules are drawn with different transparency. Selected distances (Å) and angles (°): N1–N2 1.384(2), N1–C8 1.282(3), N2–C9 1.346(3), C8–N1–N2 116.2(2), C9–N2–N1 119.8(2), C8–N1–N2–C9 4.4(2); hydrogen bonding interactions (dashed lines) as D–H, H···A, D···A, D–H···A (Å, °): O2–H···N1: 0.90(3), 1.86(3), 2.650(2), 145(2); N2–H···O4^4: 0.91(2), 1.99(2), 2.884(2), 167(2); O4–H···O3: 0.87(3), 1.82(3), 2.682(2), 169(3); O4^4–H···O2$^{4'}$: 0.85(5), 2.27(4), 3.031(3), 150(4); symmetry transformations: $4 = -x, 0.5 + y, 0.5 - z$; $4' = 1 - x, 0.5 + y, 0.5 - z$.

trans-C=N–N–C conformation and hydrogen bonding from the phenolic OH to the azomethine nitrogen atom. The phenyl rings are in plane with the central hydrazone moiety within 4.5°. Adjacent molecules are hydrogen bonded through the water molecule of crystallization. No π–π-stacking interactions with centroid–centroid contacts less than 6.0 Å and parallel π-planes could be detected [52]. The structure of $HL^1 \cdot H_2O$ can be compared to the structure of the closely related 3-methoxysalicylaldehyde 4-methoxybenzoylhydrazone monohydrate which also crystallizes in the space group $P2_12_12_1$ with similar cell constants: $a = 5.013(1)$ Å, $b = 12.733(3)$ Å, $c = 24.096(5)$ [53].

The molecular structure of $[MnCl_2(H_2O)(L^5)]$ is depicted in Fig. 2. The manganese atom is meridionally coordinated by the N,N,O donor set of the pyridin-2-yl methylene-benzohydrazide ligand. Two *cis*-coordinated chloro and aqua ligand complete the distorted pseudo-octahedral metal coordination sphere. The molecular packing is controlled by O–H···Cl and N–H···Cl hydrogen bonding with H···Cl=2.41(5)–2.43(6) Å, O/N···Cl = 3.145(4)–3.248(4) Å and O/N–H···Cl=168(4)–177(7)°. Again no π–π-stacking interactions are found [52].

3.3. Catalytic activity

For catalytic investigation we chose alkene oxidation with aim to obtain the epoxide as a target product, since

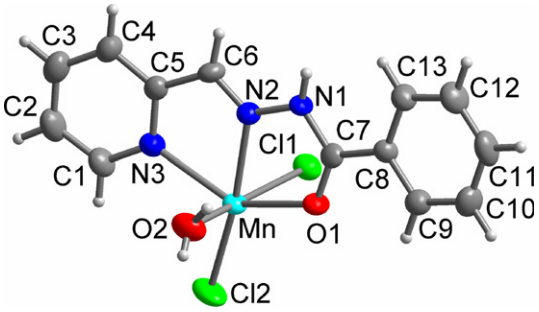

Fig. 2. Structure of $[MnCl_2(H_2O)(L^5)]$ with atom numbering. Ellipsoids are drawn with 50% probability. Selected distances (Å) and angles (°): Mn–Cl1 2.5557(14), Mn–Cl2 2.3778(13), Mn–N2 2.239(3), Mn–N3 2.321(4), Mn–O1 2.265(3), Mn–O2 2.233(4), N1–C7 1.357(6), N1–N2 1.360(4), N2–C6 1.263(5), O1–Mn–Cl1 84.39(8), O1–Mn–Cl2 118.77(9), O1–Mn–N2 69.68(11), O1–Mn–N3 139.17(11), O1–Mn–O2 82.13(13), O2–Mn–Cl1 165.50(11), O2–Mn–Cl2 96.55(10), O2–Mn–N2 86.32(13), O2–Mn–N3 85.97(14), N2–Mn–Cl1 84.00(10), N2–Mn–Cl2 171.32(10), N2–Mn–N3 70.68(12), N3–Mn–Cl1 100.90(10), N3–Mn–Cl2 101.28(10), Cl2–Mn–Cl1 94.60(5).

epoxides are one of the most useful synthetic intermediates for the preparation of oxygen-containing natural products or the production of epoxy resins, etc.

Cyclohexene is more prone to both epoxidation and allylic oxidation [54]. To provide evidence for or against nonradical mechanism and to evaluate the catalyst selectivity, oxygenation of cyclohexene was performed. The results of control experiments in oxidation of cyclohexene are shown in Table 7. The final yields, typically after 60 min are recorded. Product 2-cyclohexen-1-ol was formed in addition to the major product cyclohexene oxide. Adding a nitrogenous base like imidazole increased the conversion of substrate *and epoxide selectivity*. There is no oxidation product in the absence of catalyst. The highest substrate conversion (84%) relative to oxidant PhIO was obtained in acetonitrile with an imidazole/catalyst ratio of 10. The conversions of PhIO to the cyclohexene oxidation product were very good and the reproducibility of the reactions was excellent (±2%). The data for oxygenation of cyclohexene show more than 95% selectivity with double bond attack *in the presence of imidazole*. Approximately, most of the oxidation is occurred in the first hour of the reaction. When the reaction time was prolonged to 24 h, the yield of cyclohexene oxide was increased from 70% to 88% in experiment No. 7 (Table 7).

Marked improvements in selectivities and turnover rates have resulted from the addition of nitrogeneous bases as axial ligands such as pyridines or imidazoles to metalloporphyrin-mediated epoxidations of olefins [55,56]. In particular manganese-based catalyst systems are much improved by the use of such ligands [57,58]. The epoxidation of alkenes involving an oxo-metal intermediate spans a wide range from biomimetic oxidations catalyzed by metalloporphyrins to epoxidations catalyzed by 'designed' metal complexes, such as the metallo-salen [59]. Nitrogeneous ligands are reported to lengthen and weaken the M–O bond in the oxidized form of the catalyst by donating electron density

Table 7
Control experiments in the catalytic oxidation of cyclohexene[a]

No.	Catalyst	Axial ligand/axial ligand:catalyst ratio	Solvent	Oxidant	Conversion (%)	Epoxide yield (%)
1	none	imidazole/10	CH_3COCH_3	PhIO	0	0
2	Mn–L^3	none	CH_3CN	PhIO	46	25
3	Mn–L^3	imidazole/5	CH_3CN	PhIO	55	55
4	Mn–L^3	imidazole/10	CH_3CN	PhIO	84	84
5	Mn–L^3	imidazole/15	CH_3CN	PhIO	74	72
6	Mn–L^3	Imidazole/5	CH_3COCH_3	PhIO	67	67
7	Mn–L^3	imidazole/10	CH_3COCH_3	PhIO	70	70
8	Mn–L^3	pyridine/10	CH_3COCH_3	PhIO	45	26
9	Mn–L^3	Et_3N/10	CH_3COCH_3	PhIO	32	20

[a] Catalyst, 4.0 mg (contains 0.012 mmol Mn); oxidant PhIO, 0.5 mmol; cyclohexene, 1 mmol; imidazole/cat = 5–15 (eq); solvent 3 ml; reaction temperature, 32 ± 1 °C; reaction time, 1 h. Yields were calculated relative to the oxidant. *n*-Octane was used as internal standard, 0.175 mmol.

Table 8
Effect of imidazole/catalyst ratio and catalyst concentration on oxidation of cyclohexene[a]

Catalyst	Solvent	Imidazole/ catalyst ratio	Conversion (%)	Epoxide yield (%)
MnL^3	CH_3CN	0	43	43
MnL^3	CH_3CN	5	56	56
MnL^3	CH_3CN	10	68	68

[a] Catalyst, 2.0 mg (contains 0.006 mmol Mn); PhIO, 0.5 mmol; cyclohexene, 1 mmol; CH_3CN, 3 ml; reaction temperature, 32 ± 1 °C; reaction time, 1 h. Yields were calculated relative to the oxidant. *n*-Octane was used as internal standard, 0.175 mmol.

into the M–O antibonding orbital, which can account for the improved reactivity [60,61].

The conversion of substrate decreases with decreasing the catalyst concentration from 0.012 mmol (Table 7) to 0.006 mmol (Table 8).

The performance of the set of samples prepared as catalysts for the oxidation of cyclohexene was tested using iodosylbenzene as oxidizing reagent. In all the cases the only product observed was cyclohexene oxide *in the presence of imidazole*. The effect of various solvents for the oxidation of cyclohexene with Mn–L^{1-5} catalysts was also studied. The oxidation reactions were carried out in protic and aprotic solvents. The results are given in Fig. 3. In all the oxidation reactions, cyclohexene oxide was formed as the only product. Mn–L^2 and Mn–L^5 show low reactivity. Mn–L^1, Mn–L^3 and Mn–L^4 have comparable reactivity and Mn–L^4 showed the highest activity in the oxidation of cyclohexene with PhIO in acetonitrile, dichloromethane and acetone solvents. The efficiency of catalysts for oxidation of cyclohexene in different solvents, except for Mn–L^2, decreases in the order: dichloromethane > acetonitrile > acetone > methanol. Effect of PhIO solubility was examined. Although, homogeneous solutions of PhIO was obtained in a mixture of dichloromethane, methanol, and water (80/18/2) [62], conversion of cyclohexene did not proceed more than 48% for Mn–L^4. Although methanol has highest donor number of 30 and good polarity ($\varepsilon = 32.7$) and very easily dissolves the catalysts and PhIO, showed worst medium for catalytic oxidation of cyclohexene by these catalysts. It might be because of PhIO deactivation by methanol [63].

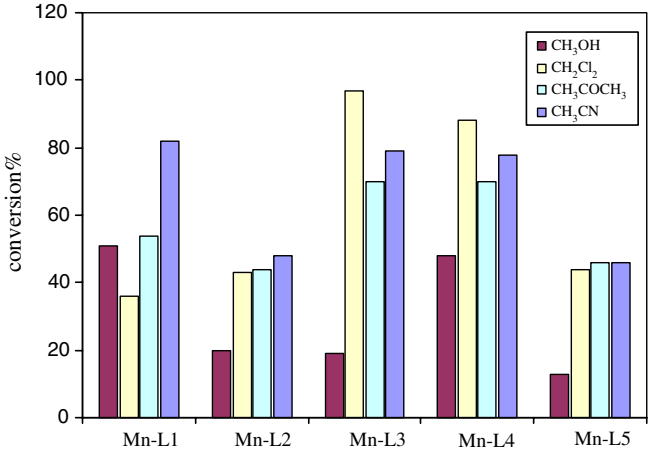

Fig. 3. Solvent effects on catalytic oxidation of cyclohexene by PhIO. Cat, 0.01 mmol; Im, 0.10 mmol, cyclohexene, 1.0 mmol; *n*-octane, 0.176 mmol; solvent, 3 ml; PhIO, 0.5 mmol; temperature, 32 °C; conversions are based on oxidant.

When the reaction was carried out in a medium coordinating solvent like CH_3CN the conversion increased. On the other hand, compared to acetone with donor number of 17.0, acetonitrile has a donor of 14.1 [64] and because it is more polar than acetone ($\varepsilon_{acetonitrile} = 37.5$, $\varepsilon_{acetone} = 20.7$), the oxidation takes place faster in this solvent.

From these results, it is evident that a polar aprotic solvent of acetonitrile with medium coordinating ability has presented the best medium for all five Mn(II) catalysts. Acetonitrile also has not environmental effect of halogenated solvent (CH_2Cl_2). The same trend was seen for the catalysts with different ratios of imidazole/catalyst or in the absence of imidazole in various solvents. In CH_3CN for imidazole/catalyst ratio = 10 the catalysts activities decreased in order (Mn–L^4, Mn–L^3, Mn–L^1) > (Mn–L^5, Mn–L^2), for oxidation in absence of imidazole, the catalysts activities decreased in order Mn–L^4 > Mn–L^3 > Mn–L^1 > Mn–L^2 > Mn–L^5.

4. Conclusion

Five new complexes of Mn(II) were prepared and characterized and crystal structures of one hydrazone Schiff

base ligand and one hydrazone Schiff base manganese complex were determined. It was demonstrated that these dissymmetric hydrazone Schiff base manganese(II) complexes (Mn–L^{1-5}) are highly selective catalysts for oxidation of cyclohexene by PhIO under mild conditions. The only product of the reaction was cyclohexene oxide *in the presence of imidazole*. Adding nitrogenous donor imidazole made catalytic activity increase. These kinds of complexes are potentially important catalysts in quantitative cyclohexene oxidation or similar oxidation processes of hydrocarbons.

Acknowledgments

We thank Zanjan University, the Deutsche Forschungsgemeinschaft through Grant JA-466/14-1 and the Fonds der Chemischen Industrie for Financial support of this study.

Appendix A. Supplementary material

CCDC 611601 and 611602 contain the supplementary crystallographic data for $HL^1 \cdot H_2O$ and $[MnCl_2(H_2O)(L^5)]$. These data can be obtained free of charge via http://www.ccdc.cam.ac.uk/conts/retrieving.html, or from the Cambridge Crystallographic Data Centre, 12 Union Road, Cambridge CB2 1EZ, UK; fax: (+44) 1223-336-033; or e-mail: deposit@ccdc.cam.ac.uk. Supplementary data associated with this article can be found, in the online version, at doi:10.1016/j.ica.2006. 08.056.

References

[1] D. Riley, M. Stern, J. Ebner, in: D.H.R. Barton, H.E. Martell, D.T. Sawyer (Eds.), The Activation of Dioxygen and Homogeneous Catalytic Oxidation, Plenum Press, New York, 1993.
[2] M. Beller, C. Bolm (Eds.), Transition Metals for Organic Synthesis, vol. 2, Wiley–VCH, Weinheim, 1998.
[3] J.M. Mitchell, N.S. Finny, J. Am. Chem. Soc. 123 (2001) 862.
[4] M.E. Nino, S.A. Giraldo, E.A. Páez-Mozo, J. Mol. Catal. A 175 (2001) 139.
[5] S.A. Patel, S. Sinha, A.N. Mishra, B.V. Kamath, R.N. Ram, J. Mol. Catal. A 192 (2003) 53.
[6] H. Hosseini-Monfared, Z. Amouei, J. Mol. Catal. A 217 (2004) 161.
[7] D. Kumar, E. Derat, A.M. Khenkin, R. Neuman, S. Shaik, J. Am. Chem. Soc. 127 (2005) 17712.
[8] A.M. Khenkin, L. Weiner, R. Neumann, J. Am. Chem. Soc. 127 (2005) 9988.
[9] R.L. Cropley, F.J. Williams, A.J. Urquhart, O.P.H. Vaughan, M.S. Tikhov, R.M. Lambert, J. Am. Chem. Soc. 127 (2005) 6069.
[10] N. Herron, Inorg. Chem. 25 (1986) 4714.
[11] R. Raja, P. Ratnasamy, Stud. Surf. Sci. Catal. 101 (1996) 187.
[12] C.R. Jacob, S.P. Varkey, P. Ratnasamy, Appl. Catal. A 168 (1998) 353.
[13] E. Armengol, A. Corma, V. Fornes, H. Garcia, J. Prince, Appl. Catal. A 181 (1999) 305.
[14] X.-H. Lu, Q.-H. Xia, H.-J. Zhan, H.-X. Yuan, C.-P. Ye, K.-X. Su, G. Xu, J. Mol. Catal. A 150 (2006) 62.
[15] (a) T. Fukuda, T. Katsuki, Tetrahedron 53 (1997) 7201;
(b) Z. Li, K.R. Conster, E.N. Jacobsen, J. Am. Chem. Soc. 115 (1993) 5326;
(c) K. Nagajima, M. Kojima, J. Fujita, Chem. Lett. (1986) 1483;
(d) Y. Yamashita, T. Katsuki, Synlett (1995) 829;
(e) J.L. Martines Leighton D.H. Carsten, E.N. Jacobsen, J. Am. Chem. Soc. 117 (1995) 5898;
(f) M. Tokunage, J.F. Larrow, F. Kakiuchi, E.N. Jacobsen, Science 277 (1997) 936.
[16] (a) E.N. Jacobsen, W. Zhang, M. Güler, J. Am. Chem. Soc. 113 (1991) 6703;
(b) E.N. Jacobsen, in: E.W. Abel, F.G.A. Stone, G. Wilkinson, L.S. Hegedus (Eds.), Comprehensive Organometallic Chemistry II, vol. 12, Pregamon Press, New York, 1995;
(c) T. Katsuki, Coord. Chem. Rev. 140 (1995) 189;
(d) K. Srinivasan, J.K. Kochi, J. Am. Chem. Soc. 108 (1986) 2309;
(e) C. Bousquet, D.G. Gilheany, Tetrahedron Lett. 42 (1995) 7739;
(f) S.-H. Zhao, P.R. Ortiz, B.A. Keys, K.G. Davenprot, Tetrahedron Lett. 37 (1996) 2752.
[17] P. Zanello, S. Tamburini, P.A. Vigato, G.A. Mazzocchin, Coord. Chem. Rev. 77 (1987) 165.
[18] M.D. Timken, W.A. Marrit, D.N. Hendrickson, R.R. Gagne, E. Sinn, Inorg. Chem. 24 (1985) 4202.
[19] T. Aono, H. Wade, Y. Aratake, N. Matsumoto, H. Okawa, J. Chem. Soc., Dalton Trans. (1995) 25.
[20] K. Ikawa, T. Nagata, K. Aruyama, Chem. Lett. (1993) 1049.
[21] I.H.A. Suez, S.O. Pehkonen, M.R. Hoffmann, Sci. Technol. 28 (1994) 2080.
[22] L.H. Terra, A.M.C. Areias, I. Gaubeur, M.E.V. Suez-Iha, Spectrosc. Lett. 32 (1999) 257.
[23] S. Patai, The Chemistry of Carbon–Nitrogen Double Bond, Interscience, New York, 1970.
[24] V. Lozan, P.-G. Lassahn, C. Zhang, B. Wu, C. Janiak, G. Rheinwald, H. Lang, Z. Naturforsch. B 58 (2003) 1152.
[25] B. Chiswell, Inorg. Chim. Acta 35 (1979) 141.
[26] B. Chiswell, J.P. Crawford, E.J. O'reilly, Inorg. Chim. Acta 49 (1980) 223.
[27] W.H. Hegazy, Monatsh. Chem. 132 (2001) 639.
[28] N.R. Sangeetha, S. Pal, S. Pal, Polyhedron 19 (2000) 2713.
[29] W. Plass, A. Pohlmann, H.-P. Yozgatli, J. Inorg. Biochem. 80 (2000) 181.
[30] R. Dinda, P. Sengupta, S. Ghosh, T.C.W. Mak, Inorg. Chem. 41 (2002) 1684.
[31] R. Raveendran, S. Pal, Polyhedron 24 (2005) 57.
[32] R.C. Elder, E.A. Blubaugh Jr., W.P. Heineman, P.J. Burke, D.R. McMillin, Inorg. Chem. 22 (1983) 2777.
[33] A.R. Amundsen, J. Whelan, B. Bosnich, J. Am. Chem. Soc. 99 (1977) 6730.
[34] K.H. Pausacker, J. Chem. Soc. (1953) 107.
[35] G. Struv, J. Prakt. Chem. 50 (1894) 295.
[36] L. Sacconi, Z. Anorg. Allg. Chem. 275 (1954) 249.
[37] SMART, Data Collection Program for the CCD Area-Detector System; SAINT, Data Reduction and Frame Integration Program for the CCD Area-Detector System. Bruker Analytical X-ray Systems, Madison, WI, USA, 1997.
[38] G. Sheldrick, Program SADABS: Area-Detector Absorption Correction, University of Göttingen, Göttingen, Germany, 1996.
[39] G.M. Sheldrick, SHELXS-97, SHELXL-97: Programs for Crystal Structure Analysis, University of Göttingen, Göttingen, Germany, 1997.
[40] DIAMOND 3.1b for Windows. Crystal Impact Gbr, Bonn, Germany. Avilable from: <http://www.crystalimpact.com/diamond>.
[41] A.L. Spek, Acta Crystallogr., Sect. A 46 (1990) C34.
[42] A.L. Spek, PLATON – A Multipurpose Crystallographic Tool, Utrecht University, Utrecht, The Netherlands, 2005.
[43] L.J. Farrugia, Windows implementation, University of Glasgow, Scotland, 2005, Version 80205.

[44] G.S. Girolami, T.B. Rauchfuss, R.J. Angelici, Synthesis and Technique in Inorganic Chemistry, third ed., University Science Books, Sausalito, 1999, p. 254.
[45] B.M. Higson, E.D. McKenzie, J. Chem. Soc., Dalton Trans. (1972) 269.
[46] R.M. Silverstein, F.X. Webster, Spectroscopic Identification of Organic Compounds, sixth ed., Wiley, New York, 1998, p. 101.
[47] K. Nakamato, Infrared and Raman Spectra of Inorganic and Coordination Compounds, fourth ed., Wiley, New York, 1986, p. 242.
[48] C.-G. Zhang, J. Sun, X.-F. Kong, C.-X. Zhao, J. Chem. Crystallogr. 29 (1999) 203.
[49] C. Boskovic, E. Rusanov, H. Stoeckli-Evans, H.U. Gudel, Inorg. Chem. Commun. 5 (2002) 881.
[50] C. Boskovic, R. Bircher, P.L.W. Tregenna-Piggott, H.U. Gudel, C. Paulsen, W. Wernsdorfer, A.-L. Barra, E. Khatsko, A. Neels, H. Stoeckli-Evans, J. Am. Chem. Soc. 125 (2003) 14046.
[51] N. Reddig, D. Pursche, M. Kloskowski, C. Slinn, S.M. Baldeau, A. Rompel, Eur. J. Inorg. Chem. (2004) 879.
[52] C. Janiak, J. Chem. Soc., Dalton Trans. (2000) 3885.
[53] Li-Hua Huo, Shan Gao, Hui Zhao, Jing-Gui Zhao, S.M. Zain, S.W. Ng, Acta Crystallogr., Sect. E 60 (2004) o1538.
[54] A.J. Appleton, S. Evans, J.R. Lindsay Smith, J. Chem. Soc., Perkin Trans. 2 (1995) 281.
[55] Z. Gross, S. Ini, J. Org. Chem. 62 (1997) 5514.
[56] J.P. Collman, J.I. Brauman, J.P. Fitzgerald, P.D. Hampton, Y. Naruta, T. Michida, Bull. Chem. Soc. Jpn. 61 (1988) 47.
[57] D. Mansuy, Pure Appl. Chem. 59 (1987) 759.
[58] D. Mohajer, S. Tangestaninejad, Tetrahedron Lett. 35 (1994) 945.
[59] (a) R.A. Sheldon (Ed.), Metalloporphyrins in Catalytic Oxidations, Marcel Dekker, New York, 1994;
(b) K. Srinivasan, P. Michaud, J.K. Kochi, J. Am. Chem. Soc. 108 (1986) 2309;
(c) D. Feichtinger, D.A. Plattner, Angew. Chem., Int. Ed. Engl. 36 (1997) 1718.
[60] A. Gold, K. Jayaraj, P. Doppelt, R. Weiss, G. Chottard, E. Bill, X. Ding, A.X. Trautwein, J. Am. Chem. Soc. 110 (1988) 5756.
[61] M.J. Gunter, P. Turner, J. Mol. Catal. A 66 (1991) 121.
[62] T.G. Traylor, J.C. Marsters, T. Nakano, B.E. Dunlap, J. Am. Chem. Soc. 107 (1985) 5537.
[63] T.G. Traylor, F. Xu, J. Am. Chem. Soc. 110 (1988) 1953.
[64] Y. Marcus, in: P.G.T. Fogg (Ed.), The Properties of Solvents, Wiley, New York, 1998.